Available online at www.sciencedirect.com
SCIENCE DIRECT
Journal of Molecular Catalysis A: Chemical 240 (2005) 40–48
JOURNAL OF MOLECULAR CATALYSIS A: CHEMICAL
www.elsevier.com/locate/molcata

Gold nanoparticles deposited on mesoporous alumina for epoxidation of styrene: Effects of the surface basicity of the supports

Donghong Yin [a,b,*], Liangsheng Qin [a], Jianfu Liu [a], Chengyong Li [a], Yong Jin [a,b]

[a] *Technology Center, Changsha Cigarette Factory, Hunan, Changsha 410014, China*
[b] *Institute of Fine Catalysis and Synthesis, College of Chem. and Chem. Eng., Hunan Normal University, Changsha 410081, China*

Received 8 April 2005; received in revised form 21 June 2005; accepted 23 June 2005
Available online 26 July 2005

Abstract

Three kinds of mesoporous alumina (denoted as *meso*-Al_2O_3-*x* (*x* = a, b, c)) supports with different surface basicity were synthesized by different structure-direct agent and different assembly pathway, respectively. The surface basicity of the *meso*-Al_2O_3-*x* and the commercial γ-Al_2O_3 was measured by means of CO_2-TPD and IR spectroscopy. The profiles of CO_2-TPD and IR spectra indicated that the mesoporous alumina owned more abundant surface basic sites than that of γ-Al_2O_3. Au nanoparticles deposited on the above supports via the method of homogeneous deposition precipitation (HDP) using urea as the precipitation agent. The supported Au catalysts were characterized by N_2 adsorption–desorption isotherms, TEM, XPS and testing the catalytic performances in the epoxidation of styrene. The dispersion and average size of the gold particles are dependent of the number of surface basic sites on the supports. Transmission electron microscopy (TEM) observations show a homogeneous distribution of gold particles lower than 4 nm on *meso*-Al_2O_3-b and *meso*-Al_2O_3-c, which owned more basic sites on the surface. XPS spectra reveal that only metallic state of Au is presented on the supports, which is independent of surface properties. The different Al_2O_3 supported Au catalysts were employed as highly active/selective and reusable catalysts for the epoxidation of styrene by anhydrous *t*-butyl hydroperoxide (TBHP). Au nanoparticles as well as the surface basic sites of the support are responsible for the epoxidation.

Keywords: Mesoporous alumina; Surface basicity; Gold; Styrene; Epoxidation

1. Introduction

Supported gold catalysts are very active in catalyzing many types of reactions like the low temperature oxidation of CO [1], oxidation of ethylene glycol [2] and D-glucose [3], the epoxidation of propene [4,5] and styrene [6,7], hydrogenation of crotonaldehyde [8] and the reduction of nitrogen oxides [9], etc. It is known that the activity of gold catalysts is related to the Au particle size, Au oxidation state and the nature of the support material. Recently, versatile methods have been reported to prepare the gold nanoparticles with high dispersion on different supports. Among the available methods, the method of deposition–precipitation is one of the most successfully used [1,10,11]. In such a preparation method, $HAuCl_4$ is used as the typical metal precursor. The chloroauric anion hydrolyzes in solution to form $[Au(OH)_nCl_{4-n}]^-$ (n = 1–4) which the interaction with the support proceeds by an anionic adsorption to precipitate gold as $Au(OH)_3$ [12–14].The surface of the support acts as a nucleating agent, and therefore the properties of the support material play a predominant role in the formation and stabilization of particle size of gold, which finally influences the catalytic activity of the resulting catalyst [10,15–19]. As a result, the isoelectric points of the supports with IEP ≈ 7, such as TiO_2 (IEP = 6), CeO_2 (IEP = 6.75) [20], ZrO_2 (IEP = 6.7) [21] and Fe_2O_3 (IEP = 6.5–6.9) [22] produce highly active catalysts. However, the acidic support, such as SiO_2 (IEP = 1–2), is found to be an unsuitable support material for gold catalysts prepared via deposition–precipitation due to the highly negatively charged surface of SiO_2 does not allow the adsorption of $[Au(OH)_nCl_{4-n}]^-$ species onto the support surface [15].

* Corresponding author. Tel.: +86 731 8872576; fax: +86 731 8872531.
E-mail address: yindh@hunnu.edu.cn (D. Yin).

1381-1169/$ – see front matter © 2005 Elsevier B.V. All rights reserved.
doi:10.1016/j.molcata.2005.06.044

Al_2O_3 (IEP = 8–9) with the amphoteric character used as a support to deposit gold has been reported as being either very active, or as expressing a certain degree of activity or even being inactive during CO oxidation at room temperature, [23,24]. For example, significant differences in the catalytic activity of CO oxidation were obtained over the gold catalysts prepared on δ-Al_2O_3 from two different supplies at the same conditions [15]. It is suggested that the physical and chemical state of the different alumina supports could influence the particles size of gold, and therefore the catalytic activity of the resulting catalysts. However, no systematic study concerning the surface basic sites of the supports on the formation of nanometer gold particles and on the catalytic activity has been published yet.

The selective and efficient epoxidation of olefins to obtain epoxides has become very important, since the epoxides are versatile intermediates in organic synthesis of fine chemicals and pharmaceuticals. Epoxidation has traditionally been carried out using peracids [25], and the procedures are very costly and usually produce huge amounts of carboxylic acids as side products. Hence, it is highly desirable to replace the conventional process with an environmentally benign procedure. Heterogeneous catalysts, such as Ti-silicalite-1 [26], Ti-β zetolite [27], Ti-SiO_2 [28], TS-2 [29] and γ-Al_2O_3 [30], are proposed as alternative catalysts because of easy separation from the reaction mixture and reusability. However, these catalysts showed either poor activity or low selectivity for the epoxides. Recently, Choudhary and co-workers have reported liquid-phase epoxidation of styrene by anhydrous *t*-butyl hydroperoxide (TBHP) over gold supported on various supports. [6,7]. They found that the activity and the epoxide selectivity were depended on Au particles size and the nature of supports.

Organized mesoporous alumina represents a very interesting molecular sieve exhibiting a narrow pore size distribution with worm-like structure, higher surface areas and abundant of surface hydroxyl groups compared to conventional alumina [31]. Recently, there are some reports regarding the formation of Au nanoparticle in the *meso*-silica and *meso*-titania [19,32–35]. However, using mesoporous alumina as a support for deposition of nanometer Au catalysts has never been reported. The objective of this work is to understand the effect of surface basicity of mesoporous alumina synthesized by different structure-direct agent on the distribution and on the size of Au nanoparticles, aiming to improve catalyst activity for liquid-phase epoxidation of styrene by anhydrous TBHP.

2. Experimental

2.1. Preparation of mesoporous alumina

The different mesoporous alumina was prepared by the following three kinds of method with different structure-directing agent.

Method A [36]: a 6.078 g of triblock poly(ethylene glycol)-poly(propylene glycol)-poly(ethylene glycol) ($EO_{20}PO_{70}EO_{20}$ (P123), BASF) together with 0.060 g $LaCl_3$ was dissolved in 25 mL sec-butanol, and then 5.4 mL aluminum sec-butoxide (Aldrich) was added with stirring. After stirring for 1 h at ambient temperature, a dilute solution of water in sec-butanol (1.14 mL H_2O/10 mL sec-butanol) was added with dropwise. The molar composition of the final reaction mixture was 0.01 La^{3+}:1.0 $Al(Bu^sO)_3$:0.10 P123:3.0 H_2O:15.5 Bu^sOH. The mixture was stirred at 45 °C for another 48 h. The product obtained was filtered, dried in air and calcined at 500 °C for 6 h in flowing air. The mesoporous alumina prepared via a neutral N^0I^0 assembly using P123 as a structure-directing agent is designed as *meso*-Al_2O_3-a.

Method B [37]: (1) a solution containing 0.8 g NaOH in 4 mL H_2O was added to 80 mL triethanolamine and heated at 120 °C for 5 min to evaporate the water. Over this solution, 21.8 mL aluminum sec-butoxide was added dropwise with stirring. The resulting solution was then heated at 150 °C for 10 min (solution I). (2) 14.56 g cetyltrimethyl ammonium bromide (CTABr, SCR) was dissolved in 240 mL H_2O at 60 °C (solution II). (3) Solution I was slowly added to solution II with vigorous stirring at 60 °C, and the mixture was allowed to age for another 72 h. The precipitate was filtered, washed with ethanol, dried at 30 °C and calcined at 500 °C for 5 h in flowing air. The mesoporous alumina prepared via an electrostatic S^+T^- pathway using CTABr as a structure-directing agent is designed as *meso*-Al_2O_3-b.

Method C: a solution of 4.60 g aluminum nitrate ($Al(NO_3)_3{\cdot}9H_20$, Fluka) dissolved in 20 mL H_2O was added to the solution of 1.50 g chitosan (DAC degree > 91.3%, viscosity 75 mPa s^{-1}, Yuhuan Ocean Biochem. Co. Ltd. China) in 50 mL of CH_3COOH solution (5%, v/v) under stirring for 1 h. And then, the mixture was added dropwise to a 800 mL of aqueous ammonia solution (50%, v/v) with vigorous stirring for 1 h. The precipitate was filtered and washed with water, dried at 30 °C for 72 h and calcined at 550 °C for 1.5 h in flowing air. The obtained mesoporous alumina by the structure-directing agent of chitosan is designed as *meso*-Al_2O_3-c.

2.2. Preparation of catalysts

meso-Al_2O_3-a, *meso*-Al_2O_3-b, *meso*-Al_2O_3-c and the commercial γ-Al_2O_3 (provided by Changling Oil Refine Corporation, calcined at 550 °C for 6 h before use) were used as the supports for deposition of gold, respectively. The supported gold catalysts were prepared by the method of homogeneous deposition precipitation (HDP) using urea as a precipitation reagent. In a typical procedure, 1 g of alumina support was added to 100 mL of an aqueous solution containing $HAuCl_4$ (9.71×10^{-3} M, 10.5 mL). The initial pH was about 4. Excess urea (Acros, p.a.) was added. The suspension was vigorously stirred and heated to 70–75 °C in order to decompose the urea. This temperature was maintained until

the pH of the solution reached gradually from 4 to 7.8. The suspension was then cooled down and filtered, washed with hot deionized water several times until no Cl^- was detected by silver nitrate solution (0.1 M) in the filtrate. The resulting Au/Al_2O_3 was dried overnight at 80 °C in air, followed by calcined in air at 330 °C for 1 h under a heating rate of 5 °C min^{-1} and then calcined at 300 °C for 0.5 h in a flow of 4% (v/v) H_2/He.

2.3. Catalyst characterization

The BET surface area and textural structure were measured by nitrogen adsorption at liquid nitrogen temperature in a Micomeritics ASAP-2400 apparatus. Before analysis, the samples were degassed 4 h at 250 °C in vacuum. The surface areas were calculated using the BET method. The isoelectric point (IEP) of alumina suspension was determined using a Brookhaven Zeta 90Plus Instruments. The ground alumina samples (0.01 wt%) were dispersed in an electrolyte solution containing 1 mM KCl as supporting electrolyte. The pH value was adjusted carefully by adding HCl (0.01 M) or NaOH (0.01 M). Zeta potential was measured following the procedures described in the instrument manual. The pH of the suspension was measured at the end of agitation to an accuracy of ±0.02 with a REX Model PHS-3C pH meter. The isoelectric points of the samples obtained by reading the intercept of the trend lines with the horizontal line of 0 mV are given in the plot of pH–zeta potential. The temperature-programmed desorption of CO_2 (CO_2-TPD) was measured in a homemade equipment with mass spectrum (Balzers Omnistar^{TM} 200) as a detector. The CO_2 adsorption temperature was 30 °C, and the temperature was ramped 500 °C at a rate of 10 °C min^{-1}. FTIR analysis was carried out using a commercial instrument (Thermo Nicolet, Avatar 370) equipped with a controlled-atmosphere chamber. The IR spectrum was measured in the reflection mode at 32 scans with a resolution of 2 cm^{-1} and corrected for the background spectrum. Pretreatment of the self-supporting wafer was performed by evacuation (10^{-2} Pa) at 573 K for 1 h. Bright-field images of transmission electron microscopy (TEM) were carried out in a JEOL JEM2010 microscope operating at 200 kV. The samples were dispersed in ethanol by sonication and dropped on a copper grid coated with a carbon film. Micrographs at various positions were taken and the size of the preferentially present particles was determined by examination of several micrographs. The average particle diameter d_s was calculated using the following formula: $d_s = \sum n_i d_i^3 / \sum n_i d_i^2$, where n_i is the number of particles of diameter d_i. At least 200 particles were chosen to determine the mean diameter of gold particles. X-ray photoelectron spectroscopy (XPS) analysis was performed using an Escalab MK2 spectrometer. The spectra were acquired using a monochromatic Mg Kα radiation source and at the pressure below 7×10^{-7} Pa. The binding energy scale was referred to the C 1s line at 284.6 eV.

2.4. Catalytic activity

The styrene epoxidation reactions over the supported Au catalysts were carried out at atmospheric pressure by contacting 0.1 g catalyst with 1.2 mL (10 mmol) styrene, 2.8 mL (15.4 mmol, Aldrich) anhydrous *t*-butyl hydroperoxide (5.5 M in decane, Fluka) and 5 mL benzene in a magnetically stirred glass reactor (capacity: 15 cm^3) at ca. 82–83 °C for 12 h. The reaction was monitored by gas chromatography with flame ionization detector (Agilent Technologies 6890N, DB-35 capillary column, 30 mm × 0.25 mm), Helium as a carrier gas, injector temperature 250 °C, the detector temperature 250 °C, oven temperature program 110 °C (2 min) → 15 °C min → 130 °C (0.5 min) → 1 °C min^{-1} → 140 °C (2 min), using dodecane as an internal standard substance. The products were identified by GC–MS using an HP5790 Series mass selective detector. The used catalyst was washed with benzene, and then it was reused for the subsequent epoxidation of styrene for testing the catalyst reusability.

3. Results and discussion

3.1. Catalyst characterization

3.1.1. Textural properties of the supports

The textural properties of the mesoporous Al_2O_3-*x* (*x* = a, b, c) and γ-Al_2O_3 were characterized by the N_2 adsorption–desorption method. The specific surface area, pore volume and the mean pore diameter of the samples are summarized in Table 1 for comparison. Obviously, the meoporous Al_2O_3 have a higher specific surface area and

Table 1
Textural properties of the supports and the supported gold catalysts[a]

Sample	BET surface area (m^2 g^{-1})	Pore volume (cm^3 g^{-1})	Mean pore diameter (nm)	IEP (pH)
meso-Al_2O_3-a	325	0.93	7.5	8.4
meso-Al_2O_3-b	302	0.78	7.2	9.4
meso-Al_2O_3-c	271	0.50	4.9	9.2
γ-Al_2O_3	108	0.43	29	8.4
Au/*meso*-Al_2O_3-a	259	0.49	4.9	–
Au/*meso*-Al_2O_3-b	355	0.59	4.3	–
Au/*meso*-Al_2O_3-c	310	0.48	4.5	–
Au/γ-Al_2O_3	92	0.46	28	–

[a] The Au loading over the support is 2.0 wt.%.

larger pore volume than that of the commercial γ-Al_2O_3. Furthermore, the specific surface area and pore volume of the mesoporous Al_2O_3 depend on the different structure-direct agent during the synthesized procedure. *meso*-Al_2O_3-a and *meso*-Al_2O_3-b obtained via the N^0I^0 assembly pathway with P123 as the structure-direct agent and the S^+T^- assembly pathway with CTABr as the structure-direct agent have a higher specific surface area, lager pore volume and wider pore diameter than that of *meso*-Al_2O_3-c prepared with chitosan as the structure-direct agent. All the samples of mesoporous Al_2O_3 have a narrow pore size distribution, but the pore size distribution of the γ-Al_2O_3 is rather broad due to the aggregate of nanosized nonporous particles.

The specific surface area, the pore volume and mean pore diameter decrease after Au particles deposited on the supports of *meso*-Al_2O_3-a and γ-Al_2O_3, which are in agreement with previously publish when gold particles are dispersed on the support of SBA-15 [32]. Interestingly, the surface areas increase as gold particles deposited on the supports of *meso*-Al_2O_3-b and *meso*-Al_2O_3-c. Somorjai and co-workers obtained the similar results when the gold nanoparticles incorporated into the silicate materials of MCM-41 and MCM-48 [33]. This is probably caused by the fact that more gold particles are small enough and arrange on the pore surface of the supports as spherical and half-spherical forms to accommodate more nitrogen molecules. On the other hand, the pore volumes and pore diameters of the samples decreased. Similar observation is obtained when organic groups are anchored onto the pore surface of MSU [38]. The difference of the surface area should be resulted from the different surface properties of the supports which leading to different Au particles size when Au species deposited on them.

3.1.2. Surface basicity measurement

From the results of the textural properties of the supports and the supported Au catalysts, we can conclude that the mesoporous Al_2O_3 and γ-Al_2O_3 should have different surface properties. Therefore, we use the means of CO_2-TPD to measure their surface basic properties. Fig. 1 shows only one asymmetric broad peak on the profiles of the four kinds of Al_2O_3. The maximum temperature of CO_2 desorption peaks are close each other and near 120 °C. Furthermore, the number of surface basic sites on the four kinds of Al_2O_3 corresponding to the areas of CO_2 desorption peaks are different. The desorption amount of CO_2 are 0.0369 mmol g^{-1} for *meso*-Al_2O_3-a, 0.0606 mmol g^{-1} for *meso*-Al_2O_3-b, 0.0503 mmol g^{-1} for *meso*-Al_2O_3-c and 0.0130 mmol g^{-1} for γ-Al_2O_3, respectively. Apparently, the mesoporous alumina with wormhole structure possesses more abundant surface basic sites owing to their high surface area. However, among the three kinds of mesoporous Al_2O_3, the support of *meso*-Al_2O_3-a with the highest surface area shows the least number of surface basic sites. This should be attributed to the different structure-directing agent used during their synthesis process. By comparing the desorption amount of CO_2, the number of surface basic sites on the mesoporous alumina follows the order of *meso*-Al_2O_3-b > *meso*-Al_2O_3-c > *meso*-Al_2O_3-a > γ-Al_2O_3. The comparison of isoelectric points value of all the supports listed in Table 1 also indicated that the surface basic properties of *meso*-Al_2O_3-b and *meso*-Al_2O_3-c are stronger than that of *meso*-Al_2O_3-a and γ-Al_2O_3.

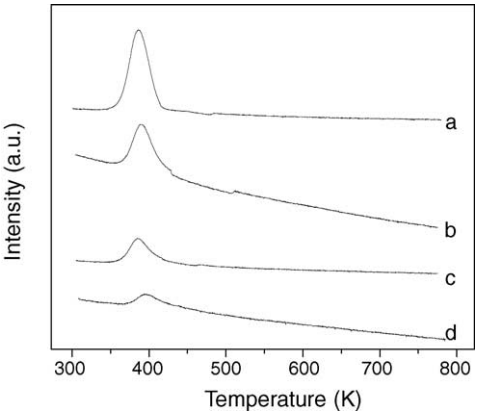

Fig. 1. CO_2-TPD profile of *meso*-Al_2O_3-b (a), *meso*-Al_2O_3-c (b), *meso*-Al_2O_3-a (c) and γ-Al_2O_3 (d).

Fig. 2 shows FTIR spectra in the region of the OH stretching mode of the different alumina samples after evacuation under vacuum at 573 K. An intense broad band centered at 3738 cm^{-1} accompanied by shoulders at the region of 3681–3618 cm^{-1} appears on the samples of mesoporous alumina. The OH band of 3738 cm^{-1} corresponding to the overlapping of bands is assigned to OH species bridging two and three Al atoms in octahedral sites as well as two Al atoms in 4- and 6-fold coordination [39], which is related to the surface basic sites. Apparently, the hydroxyl group vibration of mesoporous alumina differs from that of γ-Al_2O_3. Only a weak band centered around 3738 cm^{-1} is observed on the commercial γ-Al_2O_3. The relative intensities of the OH group vibrations of mesoporous alumina are evidently higher than those of γ-Al_2O_3, indicating that the number of surface basic

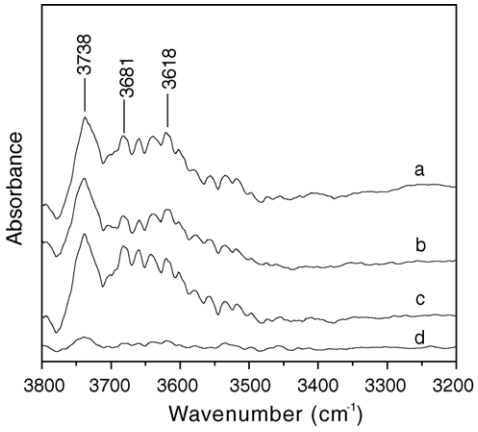

Fig. 2. IR spectra of *meso*-Al_2O_3-b (a), *meso*-Al_2O_3-a (b), *meso*-Al_2O_3-c (c) and γ-Al_2O_3 (d).

sites on the mesoporous alumina samples is greater than that on γ-Al_2O_3.

3.1.3. TEM observation

The morphology and particle size of the gold on the different Al_2O_3 supports have been determined by TEM (see Fig. 3). The gold particles are seen as dark contrasts on the surface of the supports. TEM micrographs show that the difference of the average size of the metallic gold particles with the change of supports. A homogeneous distribution of gold particles with the size of lower than 4 nm is observed all over the surface of *meso*-Al_2O_3-b and *meso*-Al_2O_3-c, which possessed more abundant surface basic sites and higher surface areas (Fig. 3b and c). The Au particles with the diameters less than 2 nm are also seen on the *meso*-Al_2O_3-b support as well as those with diameters of 3–4 nm. The average size of the gold particles on the support of *meso*-Al_2O_3-b and *meso*-Al_2O_3-c is 3.2 and 3.6 nm, respectively. However, the distributions of gold particles on supports of *meso*-Al_2O_3-a and γ-Al_2O_3 are not so uniform as that on *meso*-Al_2O_3-b even that the supports of *meso*-Al_2O_3-a has the largest surface area (Fig. 3a and d). The average size of the gold particles on the support of *meso*-Al_2O_3-a and γ-Al_2O_3 is 4.4 and 4.9 nm, respectively. This observation demonstrates that the differences in the final dispersion and average size of the metallic gold particles deposited on the surface of the four supports are mainly a consequence of their different surface basic properties, although a positive influence of a higher surface area of the supports cannot be ruled out. The more the number of the surface basic sites has, the better of the gold particles distribution and the smaller of the mean diameter are obtained.

It is known that with increasing the basicity of supports, the pH at the support solution interface is increased, resulting in more precipitation of hydroxylated gold species on the support surface due to an increase of OH^- ion concentration at the interface [15]. The OH^- ions on the surface of support can exchange the chloride ions in the species of $[Au(OH)_nCl_{4-n}]^-$ (n = 1–4) to decrease the residual Cl^- and to form $[AuCl(OH)_3]^-$ precursor, resulting in small and high dispersion of gold particles on the supports. Furthermore, in the preparation of Au/Al_2O_3 catalysts by HDP method, the gradual and homogenous addition of hydroxide ions throughout the solution avoids local increasing in pH value in the solution, which is always below the IEP value of the supports. It can be inferred that the surface-charged alumina support is always positive, which should be in favor of attracting negatively charged species of $[Au(OH)_nCl_{4-n}]^-$ (n = 1–4) in solution, especially for the complex of $[AuCl(OH)_3]^-$. The obtained average gold particle size should be smaller at the surface of the support with higher IEP value. Therefore, the supports of *meso*-Al_2O_3-b and *meso*-Al_2O_3-c with more number of the surface basic sites are advantageous for the formation and stabilization of small gold particles. Combining with the results of surface areas and IEP value of the supports obtained in Table 1, as well as the determination of surface basicity in Fig. 1, it is proposed that the gold particles size and distribution on the different Al_2O_3 supports are mainly affected by their surface basicity.

3.1.4. XPS characterization

Although the catalytic activity of gold catalysts in the low temperature CO oxidation has been intensively studied during the last decade, the nature of the active species is still discussed controversially. It has been suggested that the role of the metal oxide is the stabilization of the gold nanoparticles and that the reaction takes place on the gold surface [1]. Some authors proposed that the reaction takes place at the gold/metal oxide interface and that the metal oxide could act as a source of oxygen [16]. Also the electronic structure of gold in active catalysts is unclear, but most of other authors suggest metallic gold to be the active species. The XPS spectra of the Au 4f (region Au $4f_{7/2}$ and Au $4f_{5/2}$) are employed to investigate the state of gold on the different supports. The results indicated that only a binding energy of 83.8 eV for the Au $4f_{7/2}$ electron and 87.5 eV for the Au $4f_{5/2}$ electron (Δ = 3.7 eV) with the change of supports for the fresh samples. The binding energy indicates exclusively $Au^{(0)}$-particles without any trace of higher oxidized species on the four kinds of Al_2O_3 surface. The surface basicity of the support has no effect on the state of gold if the Au catalysts prepared at the same conditions.

3.2. Catalytic properties

3.2.1. Effect of supports

Table 2 summarizes the results of epoxidation of styrene using anhydrous TBHP as an oxidizing agent over Au catalysts supported on different Al_2O_3. The effect of supports on the conversion of styrene and the selectivity of the styrene oxide was investigated. As can be seen from this table, the epoxidation of styrene is very slow in the absence of catalyst. However, the different support of Al_2O_3 used as a catalyst shows the different catalytic activity, which is different from the reports of Choudhary and co-workers [7]. They did not find apparently conversion of styrene over Al_2O_3 support. Our results suggest the surface basic sites of the supports facilitating to the epoxidation should not be ruled out completely. Furthermore, the catalytic activity increased with increasing the surface basicity of the supports. Kirm et al. also observed that the basic sites of hydrotalcites with different atomic ratio of Mg/Al play an important role in the epoxidation of styrene [40], and also the catalytic activity increased with the surface Brösted basic sites.

For the Au/*meso*-Al_2O_3-a, Au/*meso*-Al_2O_3-b, Au/*meso*-Al_2O_3-c and Au/γ-Al_2O_3 catalysts, the difference of selectivity to styrene oxide is not significant. However, the catalytic activity follows the order of Au/*meso*-Al_2O_3-b > Au/*meso*-Al_2O_3-c > Au/*meso*-Al_2O_3-a > Au/γ-Al_2O_3, which is coincident with the Au particle size and the surface basic sites on the supports. The catalyst of Au/*meso*-Al_2O_3-b shows 84.3% of conversion, which is higher than that the results obtained over the catalyst of Au/Al_2O_3 in the reference [7]. It should be

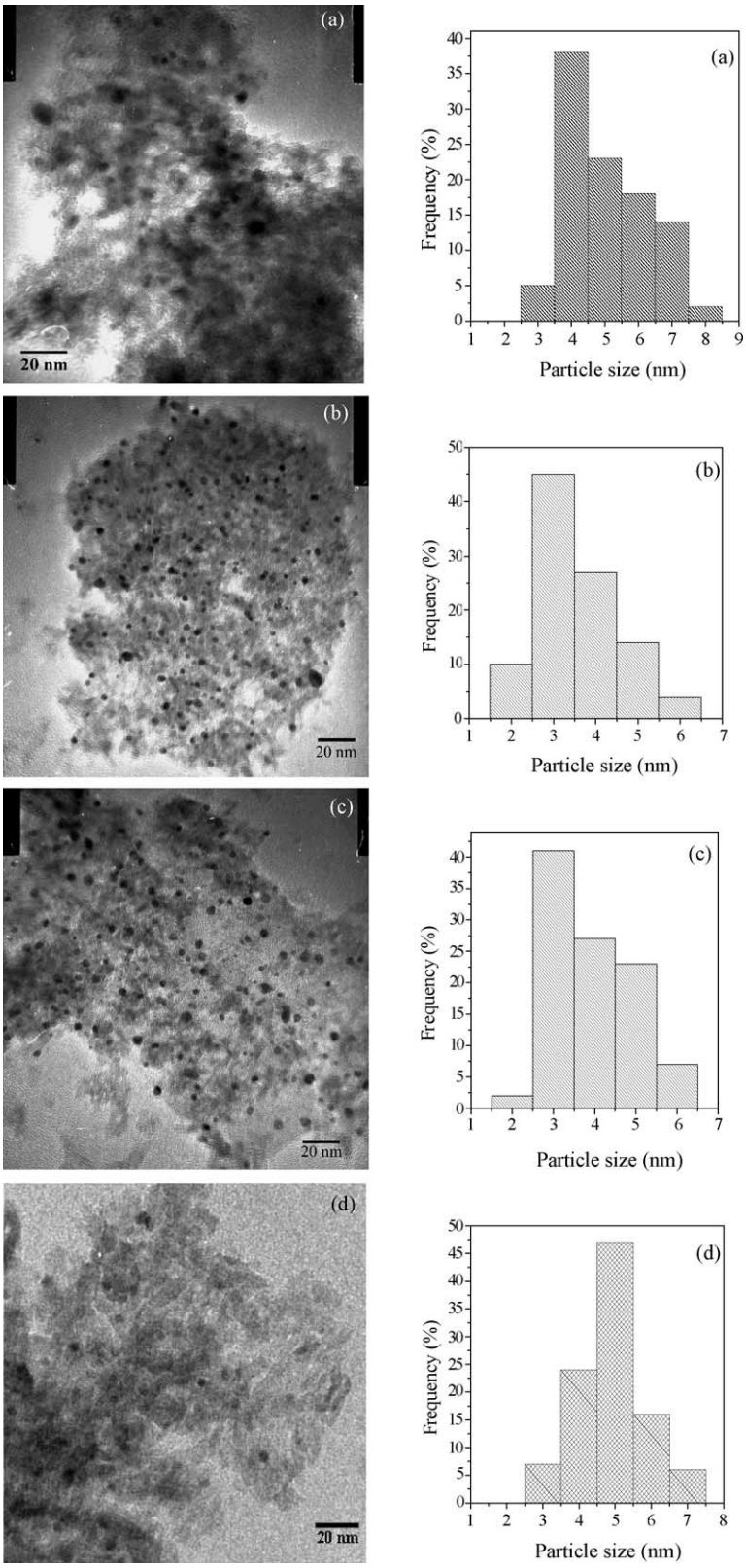

Fig. 3. TEM micrographs and size histogram of Au particles supported on *meso*-Al_2O_3-a (a), *meso*-Al_2O_3-b (b), *meso*-Al_2O_3-c (c), and γ-Al_2O_3 (d).

Table 2
Performance of Au catalyst with different supports in styrene epoxidation[a]

Catalysts	Styrene conversion (%)	Selectivity (%)			
		Styrene oxide	Benzaldehyde	Phenyl acetaldehyde	Others[b]
No	8.3	75.9	14.6	4.7	4.8
meso-Al_2O_3-a	38.6	65.0	18.0	5.2	11.8
meso-Al_2O_3-b	50.3	66.9	21.0	5.2	6.9
meso-Al_2O_3-c	43.8	65.8	20.1	2.0	12.1
γ-Al_2O_3	36.0	69.9	16.4	4.7	9.0
Au/*meso*-Al_2O_3-a	71.1	65.6	24.5	6.4	3.5
Au/*meso*-Al_2O_3-b	84.3	69.0	23.0	3.6	4.4
Au/*meso*-Al_2O_3-c	76.1	67.4	22.3	5.5	4.7
Au/γ-Al_2O_3	64.5	67.8	25.6	3.3	3.3

[a] The reaction was performed at 82 °C for 12 h over 0.10 g of the supported catalyst with 2.0% of Au loading.
[b] Others are benzoic acid and phenyl acetic acid.

Table 3
The effect of Au loading on the epoxidation of styrene[a]

Gold loading (%)	Styrene conversion (%)	Selectivity (%)			
		Styrene oxide	Benzaldehyde	Phenyl acetaldehyde	Others[b]
1.0	68.5	74.7	19.3	3.6	2.4
2.0	84.3	69.0	23.0	3.6	4.4
3.5	100	60.3	30.1	3.6	6.0
5.0	100	58.8	28.0	4.0	9.2

[a] The reaction was performed at 82 °C for 12 h over 0.10 g of the supported catalyst.
[b] Same as in Table 2.

attributed to more homogeneous distribution and the smaller average Au particle size (3.1 nm) in our experimental. It is known that the epoxidation activity of the supported gold catalysts is mainly attributed to the low coordinated Au atoms at the corners and edges of nanosize gold particles even that the catalytic reaction mechanism is not yet clear [6,7]. Therefore, the small Au particles are presented homogeneously on the surface of the support should exhibit the high activity for the epoxidation of styrene. The smaller size of Au particles is, the higher catalytic activity can be obtained. Therefore, both the Au nanoparticles and the surface basic sites of the supports can catalyze the epoxidation of styrene, but the Au particles dispersed homogeneously onto support with small particle size should play major role for the epoxidation.

3.2.2. Effect of Au loading

Table 3 summarizes the results of epoxidation of styrene over the catalyst of Au/*meso*-Al_2O_3-b at various Au loading. It is expected that the conversion of styrene increased with an increase of the Au loading. However, the selectivity to styrene epoxide decreased due to the increase of benzaldehyde selectivity. When Au loading is up to 3.5 wt%, the conversion of styrene is up to 100%, but the selectivity of benzaldehyde, benzoic acid and phenyl acetic acid increase. These results indicate that Au nanoparticles on the support of Al_2O_3 are the main active sites for the epoxidation of styrene.

3.2.3. Effect of water

It is significant that the activity of Au nanoparticles is sensitive to the water content on the catalyst. Haruta and co-workers reported that the activity of the Au/TiO_2 catalyst for CO oxidation is mainly affected by the amount of moisture adsorbed on the catalyst [41]. They found that the suppression of the reaction by the excess amount of water could be explained by blocking of the active sites. A series of experiments is carried out using Au/*meso*-Al_2O_3-b as a catalyst to examine the effect of water content on the catalytic properties. The results are shown in Fig. 4. It can be seen that the conversion of styrene and selectivity of styrene oxide remain almost unchanged with addition of water less than 2%. The results suggest that the low concentration of water

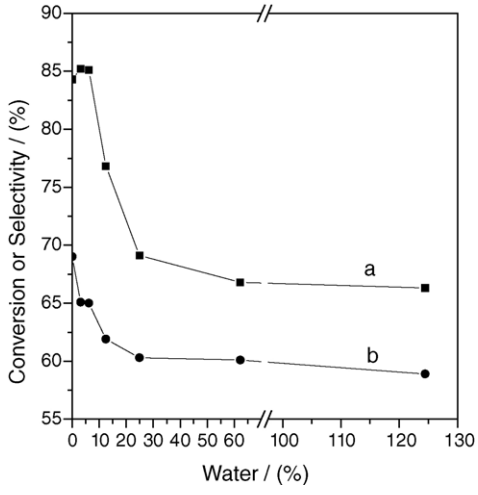

Fig. 4. Effect of amounts of water on conversion of styrene (a) and selectivity of styrene oxide (b).

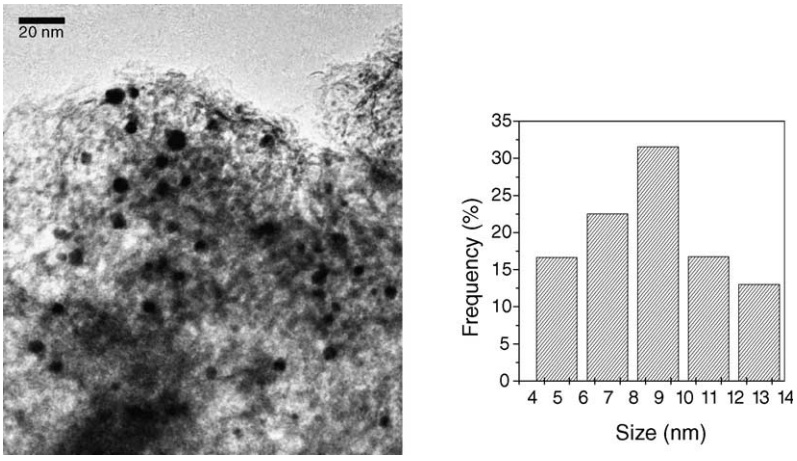

Fig. 5. TEM micrographs and size histogram of Au particles in the catalyst of Au/*meso*-Al_2O_3-b separated from reaction by addition of 20% water.

in the reaction has not significant effect on the catalytic activity and selectivity. With an increase of water content from 5 to 20%, the catalytic activity decreases (from 84 to 72%). In this case, the color of the catalyst turned from wine to pink, which is suggested that high content of water result in aggregation of Au particles on the support. It was confirmed by the TEM image of the Au/Al_2O_3-b catalyst (Fig. 5), where the catalyst was separated from the reaction system with addition of 20% water and then dried at 80 °C in vacuum. It is observed that the gold particles become large with the average gold particle size of 8.7 nm. Only 70% of conversion was obtained if the dried catalyst was used again. The lost activity is attributed to the adsorption of water on the catalyst leading the unstable small Au nanoparticles to aggregate together. When the content of water exceeds 25%, the change of conversion of styrene and the selectivity of styrene oxide are not apparent. In this case, the remained activity of the catalyst is mainly from the surface basic sites.

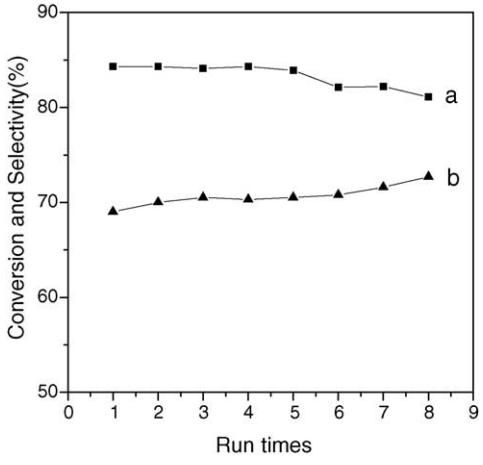

Fig. 6. Effect of Au/*meso*-Al_2O_3-b reuse on the conversion of styrene (a) and selectivity of styrene oxide (b).

3.2.4. *Reuse of the catalyst*

The used catalyst of Au/*meso*-Al_2O_3-b was washed with benzene, and then reused for the subsequent epoxidation of styrene. The above procedure was repeated for eight times and the results are shown in Fig. 6. It was observed that there was no noticeable decrease in activity even up to five subsequent runs. Only 3% catalytic activity (from 84 to 81%) is lost after the catalyst reused nine times. Interestingly, the trend of the selectivity of styrene oxide increases slightly. These results indicate that the catalyst is relatively stable in the epoxidation of styrene using anhydrous TBHP as an oxidant.

4. Conclusions

The surface basic sites on the support of mesoporous Al_2O_3 influence the final dispersion and average size of the obtained gold particles during the homogeneous deposition–precipitation process. The more number of the surface basic sites are advantageous for to form uniform and smaller size of Au nanoparticles. The supported nanometer Au catalyst shows high catalytic activity and selectivity for the liquid-phase epoxidation of styrene by anhydrous *t*-butyl hydroperoxide. Smaller size of Au particles and surface basic sites on the support are responsible for the catalytic reaction. Due to the possibility to separate easily and reuse in the reaction, the gold nanoparticles supported on *meso*-Al_2O_3-b should be a promising heterogeneous catalyst for the epoxidation of alkylene.

Acknowledgements

The project was sponsored by the Scientific Research Foundation for the Returned Overseas Chinese Scholars, State Education Ministry [2003-406].

References

[1] M. Haruta, S. Tsubota, T. Kobayashi, H. Kageyama, M.J. Genet, B. Delmon, J. Catal. 144 (1993) 175.
[2] H. Berndt, I. Pitsch, S. Evert, K. Struve, M.-M. Pohl, J. Radnik, A. Martin, Appl. Catal. A 244 (2003) 169.
[3] Y. Önal, S. Schimpf, P. Claus, J. Catal. 223 (2004) 122.
[4] T. Hayashi, K. Tanaka, M. Haruta, J. Catal. 178 (1998) 566.
[5] E.E. Stangland, K.B. Stavens, R.P. Andres, W.N. Delgass, Stud. Surf. Sci. Catal. 130 (2000) 827.
[6] N.S. Patil, B.S. Uphade, P. Jana, S.K. Bharagava, V.R. Choudhary, J. Catal. 223 (2004) 236.
[7] N.S. Patil, R. Jha, B.S. Uphade, S.K. Bhargava, V.R. Choudhary, Appl. Catal. A 275 (2004) 87.
[8] R. Zanella, C. Louis, S. Giorgio, R. Touroude, J. Catal. 223 (2004) 328.
[9] T. Salama, R. Ohnishi, T. Shido, M. Ichikawa, Chem. Commun. (1997) 105.
[10] G.C. Bond, D.T. Thompson, Catal. Rev. Sci. Eng. 41 (1999) 319.
[11] S. Tsubota, D.A. Cunningham, Y. Bando, M. Haruta, in: G. Poncelet, et al. (Eds.), Preparation of Catalysts, vol. VI, Elsevier, Amsterdam, 1995, pp. 227–235.
[12] S. Ivanova, C. Petit, V. Pitchon, Appl. Catal. A 267 (2004) 191.
[13] H.H. Kung, M.C. Kung, C.K. Costello, J. Catal. 216 (2003) 425.
[14] M.Á. Centeno, I. Carrizosa, A. José, Odriozola, Appl. Catal. A 246 (2003) 365.
[15] A. Wolf, F. Schüth, Appl. Catal. A 226 (2002) 1.
[16] M.M. Schubert, S. Hackenberg, A.C. van Veen, M. Muhler, V. Plzak, R.J. Behm, J. Catal. 197 (2001) 113.
[17] J.-D. Grunwaldt, M. Maciejewski, O.S. Becker, P. Fabrizioli, A. Baiker, J. Catal. 186 (1999) 458.
[18] K. Mallick, M.J. Witcomb, M.S. Scurrell, J. Mol. Catal. A 215 (2004) 103.
[19] W. Yan, B. Chen, S.M. Mahurin, E.W. Hagaman, S. Dai, S.H. Overbury, J. Phys. Chem. B 108 (2004) 2793.
[20] D. Andreeva, V. Idakiev, T. Tabakova, L. Ilieva, P. Falaras, A. Bourlinos, A. Travlos, Catal. Today 72 (2002) 51.
[21] A. Knell, P. Barnickel, A. Baiker, A. Wokaun, J. Catal. 137 (1992) 306.
[22] M. Haruta, N. Yamada, T. Kobayashi, S. Ijima, J. Catal. 115 (1989) 301.
[23] R.J.H. Grisel, B.E. Nieuwenhuys, J. Catal. 199 (2001) 48.
[24] S.J. Lee, A. Gavriilidis, J. Catal. 206 (2002) 305.
[25] D. Swen, in: R. Adams (Ed.), Organic Reactions, Wiley, New York, 1953, p. 378.
[26] M. Taramasso, G. Perego, B. Notari, US Patent, 4,410,501 (1983).
[27] A. Camblor, A. Corma, A. Martĭýnez, J. Pérez-Pariente, J. Chem. Soc., Chem. Commun. (1992) 583.
[28] Q. Yang, S. Wang, J. Lu, G. Xiong, Z. Feng, X. Xin, C. Li, Appl. Catal. A 194–195 (2000) 507.
[29] Z. Fu, D. Yin, D. Yin, Q. Li, L. Zhang, Y. Zhang, Microporous Mesoporous Mater. 29 (1999) 351.
[30] V.R. Choudhary, N.S. Patil, S.K. Bhargava, Catal. Lett. 89 (2003) 55.
[31] S.A. Bagshaw, T.J. Pinnavaia, Angew. Chem. Int. Ed. Engl. 35 (1996) 1102.
[32] C.M. Yang, M. Kalwei, F. Schüth, K.J. Chao, Appl. Catal. A 254 (2003) 289.
[33] Z. Ko'nya, V.F. Puntes, I. Kiricsi, J. Zhu, J.W. Ager, M.K. Ko, H. Frei, P. Alivisatos, G.A. Somorjai, Chem. Mater. 15 (2003) 1242.
[34] H. Araki, A. Fukuoka, Y. Sakamoto, S. Inagaki, N. Sugimoto, Y. Fukushima, M. Ichikawa, J. Mol. Catal. A 199 (2003) 95.
[35] J.J. Pietron, R.M. Stroud, D.R. Rolison, Nano. Lett. 2 (2002) 545.
[36] W. Zhang, J. Pinnavaia, Chem. Commun. 11 (1998) 1185.
[37] S. Cabrara, J.E. Haskouri, J. Alamo, A. Beltran, D. Beltran, S. Mendioroz, M.D. Marcos, P. Amoros, Adv. Mater. 11 (1999) 379.
[38] N. Yu, Y. Gong, D. Wu, Y. Sun, Q. Luo, W. Liu, F. Deng, Microporous Mesoporous Mater. 72 (2004) 25.
[39] V. González-Peña, I. Díaz, C. Márquez-Alvarez, E. Sastre, J. Pérez-Pariente, Microporous Mesoporous Mater. 44–45 (2001) 203.
[40] I. Kirm, F. Medina, X. Rodriguez, Y. Cesteros, P. Salagre, J. Sueiras, Appl. Catal. A 272 (2004) 175.
[41] M. Date, M. Haruta, J. Catal. 201 (2001) 221.